

# Reactive deposition of ultrafine cobalt powders

## Part I *Electrochemical investigation*

C. Q. CUI

*Department of Chemical Engineering, National University of Singapore, 10 Kent Ridge Crescent, Singapore 0511*

A. C. C. TSEUNG\*

*Chemical Energy Research Centre, Department of Chemistry and Biological Chemistry, University of Essex, Wivenhoe Park, Colchester CO4 3SQ, UK*

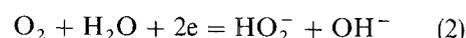
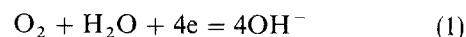
During the reactive deposition of cobalt powders,  $\text{Co(OH)}_2$  colloidal layers are formed at the electrode surface; the individual cobalt crystals are isolated by the  $\text{Co(OH)}_2$  colloid around the grain boundaries so that their growth is inhibited and ultrafine cobalt crystal grains are formed, which are loosely attached to the titanium substrate. The existence of  $\text{Co(OH)}_2$  colloid layer at the electrode surface depresses the hydrogen evolution reaction in the deposition process and accelerates the decrease of the interfacial  $\text{Co}^{2+}$  concentration. Therefore, compared to the normal deposition of cobalt powders, it has several unique advantages: (1) ultrafine cobalt powders (0.4–0.6  $\mu\text{m}$ ) can be produced; (2) the amount of  $\text{Co(OH)}_2$  in the powders is decreased; (3) there is a wider range of current density for the formation of cobalt powders.

### 1. Introduction

Cobalt and cobalt alloys are widely employed in corrosion protection, catalysis, batteries, and as the recording media in both magnetic drum and magnetic tape memory systems in the computer [1, 2]. Moreover, the manufacture of hard metal tools, grinding and polishing materials is currently estimated to consume 10%–15% of the western worlds' cobalt production [3]. At present, cobalt powder production involves the pyrolysis of an organic cobalt salt under reducing conditions, followed by further mechanical grinding. Because all the above applications require fine cobalt powders, an alternative inexpensive method for producing such powders is of considerable interest. One possible alternative approach is to produce the powders electrically [4]. Electrolytic metal powders are produced industrially by two procedures [4]. Deposition of the powder directly on the cathode, stripping the deposited coating, and grinding a partially coherent but brittle deposit; and the electrodeposition of cobalt powder from  $\text{CoSO}_4$  solutions [5], but in this case the products are contaminated by significant amounts of  $\text{Co(OH)}_2$  and the particle size of the products is larger than that produced via the pyrolysis route.

Reactive deposition is a novel process involving the deposition of metal in the presence of bubbling oxygen and the presence of  $\text{Cl}^-$  ions in solution [6, 7]. The mechanism and kinetics of the reactive deposition of cobalt have been extensively studied in the presence of bubbling oxygen and dissolved oxygen [8–13]. The

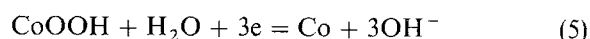
preparation of active plates in rechargeable batteries by reaction deposition has also been reported [14]. In the reactive deposition of cobalt, oxygen is reduced prior to the deposition of cobalt through a four- and a two-electron process in unbuffered neutral solutions.



A  $\text{Co(OH)}_2$  colloid layer is formed in the vicinity of the electrode surface, by reaction with the  $\text{OH}^-$  formed in Reactions in 1 and 2 [11–13]



The formation of such a poorly conductive  $\text{Co(OH)}_2$  colloid layer inhibits the deposition of cobalt and depresses the nucleation potential to the cathodic side, increasing the nucleation rate of the deposition. Moreover, the product of the oxygen reduction,  $\text{HO}_2^-$ , reacts with the  $\text{Co(OH)}_2$  colloid layer at the electrode surface to form the electroactive species,  $\text{CoOOH}$ , which is then further reduced to form cobalt metal.



In addition, the mechanical sparging of bubbling oxygen has a significant effect on the stability of the  $\text{Co(OH)}_2$  colloid layer. Therefore, the dynamic states, i.e. the formation and breakdown processes of the  $\text{Co(OH)}_2$  colloid layer, are responsible for the formation of high surface area and a highly porous (i.e.

\* Author to whom all correspondence should be addressed.

ultrafine crystal) cobalt deposit. Reactive deposition of cobalt is characterized by localized nucleation and limited crystal growth processes. It has been found by scanning electron microscopy that the deposit prepared by reactive deposition shows the existence of fine ( $\sim 0.1 \mu\text{m}$ ) and coarse pores ( $\sim 1 \mu\text{m}$ ), together with similar sized fine and coarse pores. As a result, the reactive deposition method offers the possibility of manufacturing ultrafine cobalt powders. In the present work, the electrochemical characteristics of the reactive deposition of cobalt powders were studied and the effect of oxygen in the electrolyte solution on the formation of cobalt powders analysed and compared to the normal electrolytic manufacture of cobalt powders. In Part II of this paper, the physical properties of the reactively deposited cobalt powders will be measured and its practical application discussed.

## 2. Experimental procedure

The deposition of cobalt was carried out in an electrolytic cell as described by Jiang *et al.* [8]. The volume of the electrolyte was 220 ml. Gas (oxygen or nitrogen) was fed through a sintered glass plug directly on to the working electrode and the flow rate of the gas was monitored. Titanium foil was used as the metal substrate in this study to facilitate the easy collection of cobalt powder. Titanium foil was placed in boiling dilute HCl for 10 min to clean the oxidized layer on the surface, then washed with distilled water, dried with tissue paper and subsequently kept in anhydrous alcohol until use. The apparent surface area of the titanium foil substrate was  $1 \text{ cm}^2$ . Cobalt metal (99.5% Co, Cobalt Development Institute) was used as the counter electrode. The deposition potential was measured against a SCE reference electrode. The electrolyte was made from  $\text{CoCl}_2$  (Analar Grade, BDH) and distilled de-ionized water. Prior to the deposition, either nitrogen or oxygen was bubbled through the electrolyte for 10 min ( $30 \text{ ml min}^{-1}$ ) to ensure that the electrolyte was either oxygen-free or saturated with oxygen.

The deposition was controlled by an Oxford Electrode rotating disc assembly. The experimental results were plotted on a recorder (Lloyd, PL2500). All experiments were performed at room temperature. The morphology of the cobalt deposit on the titanium foil was examined by scanning electron microscopy.

## 3. Results and discussion

### 3.1. Deposition of powdery cobalt in the presence of bubbling nitrogen

Fig. 1 gives the potential-time transients without correction of the ohmic drop between the working and reference electrodes obtained from  $0.05 \text{ M CoCl}_2$  solution at different current densities in the presence of bubbling nitrogen ( $30 \text{ ml min}^{-1}$ ). At a current density of  $20 \text{ mA cm}^{-2}$ , the potential decreases with time. Similar behaviour has also been found in previous studies [15]. Once powder deposition has started, the surface area of the electrode increases and the real current density is smaller than that based on the

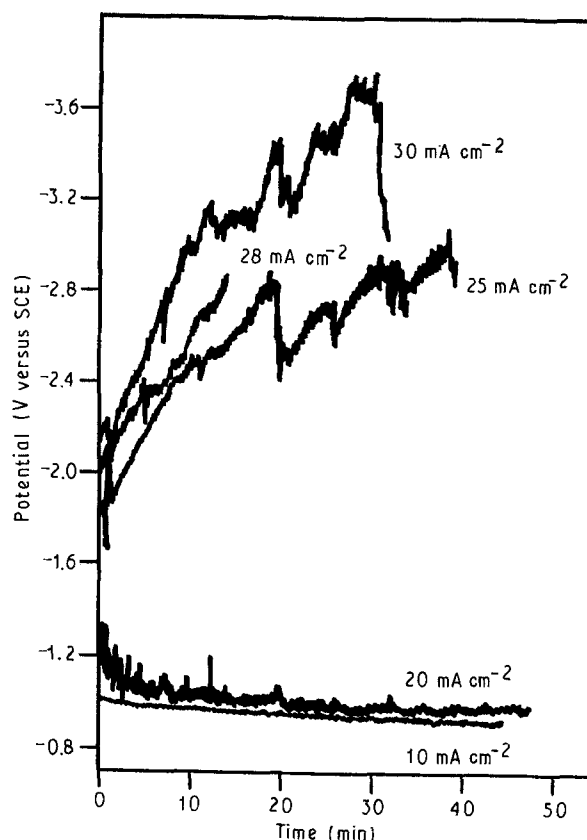


Figure 1 Potential-time transient curves obtained from  $0.05 \text{ M CoCl}_2$  solution on a titanium substrate at different current densities in the presence of bubbling nitrogen ( $30 \text{ ml min}^{-1}$ ) without the correction of ohmic drop.

geometric area. At this current density, the colour of the deposit obtained is black, indicative of the formation of cobalt powder which can be collected by scraping the deposit from the titanium substrate. However, when the current density is lower than  $10 \text{ mA cm}^{-2}$ , grey and dense deposits are formed and no powder is obtained.

In contrast, when the current densities are higher than  $20 \text{ mA cm}^{-2}$ , the potential increases rapidly with time. The deposit obtained in this case is green, which is indicative of a large amount of  $\text{Co(OH)}_2$  in the deposit. As in the case of nickel and iron deposition, hydrogen evolution also occurs during the deposition of cobalt. At such high current density, hydrogen evolution is probably the main electrode reaction in unbuffered neutral solution and the concentration of  $\text{Co}^{2+}$  on the electrode surface is not high enough to sustain high rates of cobalt deposition. The rapid increase in pH caused by hydrogen evolution results in the precipitation of  $\text{Co(OH)}_2$  which is co-deposited with cobalt in the vicinity of the electrode. The poor conductivity of  $\text{Co(OH)}_2$  leads to a rapid increase in potential and an incoherent deposit is obtained after the appearance of  $\text{Co(OH)}_2$  in the electrolyte. Similar observations have been reported in the electrodeposition of iron group metal powder. In order to decrease the change in pH at the electrode surface, pH buffer is generally added: for example, solutions of  $\text{FeCl}_2$  with the addition of  $\text{NH}_4\text{Cl}$  have been found to be very suitable [16].

Therefore, it can be seen from Fig. 1 that the range of current density for the formation of cobalt powder

is greatly limited by the accompanying hydrogen evolution in the unbuffered neutral solution in the absence of oxygen. In 0.05M CoCl<sub>2</sub> solution at a nitrogen flow rate of 30 ml min<sup>-1</sup>, the only suitable current range for the formation of cobalt powder is 10–20 mA cm<sup>-2</sup>.

The potential–time transients in the initial deposition region of Fig. 1 are shown in Fig. 2a. Due to stirring and the shielding interference of nitrogen bubbles, it is very difficult to analyse the kinetics of the deposition processes. One effective way to avoid the interference is to outgas the dissolved oxygen by bubbling nitrogen through the electrolyte before the experiment. Fig. 2b shows the transients from 0.05M CoCl<sub>2</sub> solution in the absence of oxygen. The common characteristic of the all transients in Fig. 2 is that the overpotential increases and reaches a plateau after some time. At short deposition times, because the change in surface area of the electrode is less with respect to the change in the concentration on the electrode surface, the potential–time transients mainly

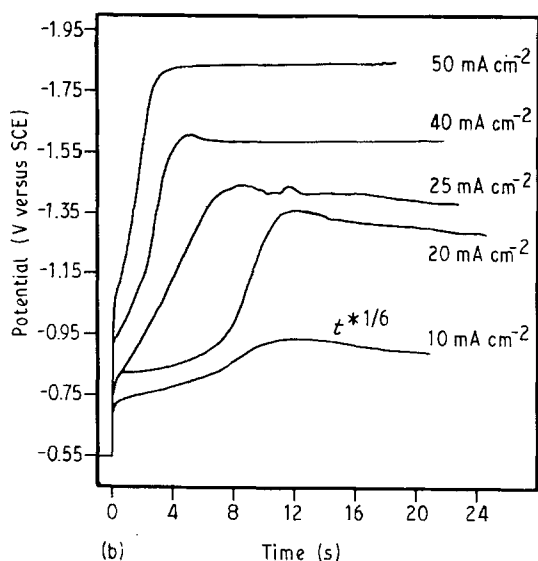
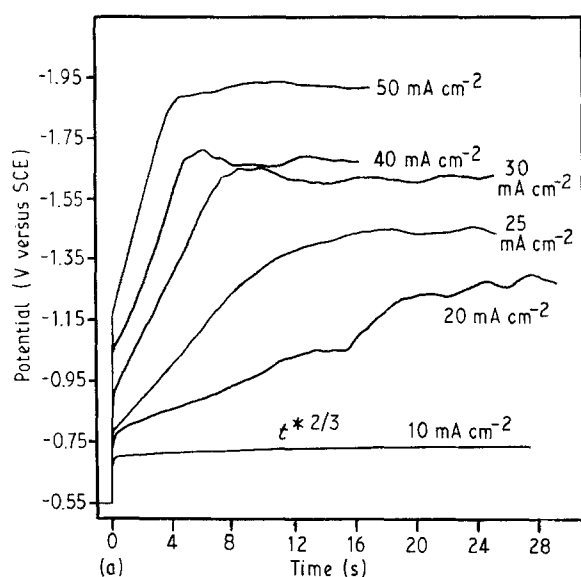


Figure 2 Potential–time transient curves in the initial deposition obtained from 0.05M CoCl<sub>2</sub> solution (a) in the presence of bubbling nitrogen (30 ml min<sup>-1</sup>) and (b) in the absence of oxygen, respectively.

reflect the characteristic changes in the concentration of metal ions at the electrode surface. At a constant current density, because of the depletion of the interfacial Co<sup>2+</sup> concentration, the overpotential increases so that hydrogen evolution becomes the main reaction. Under such conditions, the overpotential will not change with time. Therefore, the occurrence of the potential plateau in Fig. 2 indicates that the limiting current density for cobalt deposition has been reached. At constant current density, in the absence of convection, the interfacial concentration decreases continuously with time. The relationship between the interfacial concentration with the current,  $i$  and the time  $t$ , is given by [4]

$$it^{1/2} = [zF/2(1 - n_c)](C_o - C_e)(\pi D)^{1/2} \quad (6)$$

where  $z$  is the electron number exchanged per one metal ion in the reaction,  $F$  is the Faraday constant,  $n_c$  the transference number of the depositing metal cation,  $D$  the diffusion coefficient of the metal ion in the aqueous solution,  $C_o$  and  $C_e$  the concentration of the metal ions at the electrode surface and in the bulk of solution, respectively.  $C_e = 0$  when the deposition is at the transition time. As an illustration, the time,  $t_1$ , to reach the potential plateau, measured in Fig. 2, is plotted logarithmically against current density in Fig. 3. A straight line with a slope of approximately  $-2$  is obtained as required by Equation 6. Therefore, this means that the time to reach the potential plateau in Fig. 2 may be reasonably considered as the transition time when the interfacial concentration falls to zero.

On the other hand, in our previous studies [12], it has been confirmed that the main effect of gas sparging, where nitrogen is generally used, is to increase the mass transfer process and therefore the limiting current density, and bubbling nitrogen has little effect on the nucleation potential for the electrodeposition of cobalt. As shown in Fig. 3, the transition time is longer at a constant current density for the deposition of cobalt in the presence of bubbling nitrogen, compared to the absence of bubbling nitrogen. At low current density, the transition time is never reached

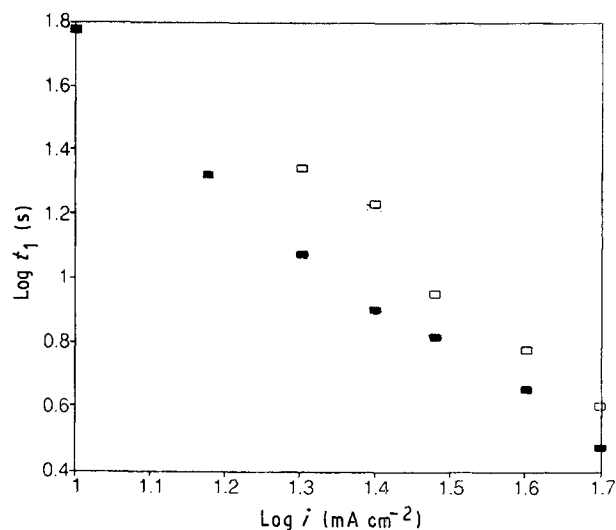


Figure 3 Logarithmical relationship of current density with the transition time measured from 0.05M CoCl<sub>2</sub> solution. (■) with bubbling nitrogen, (□) without oxygen.

because forced or natural convection prevents the interfacial concentration from decreasing to zero. After some time a steady state is established in which the interfacial concentration is independent of time. Therefore, in the presence of bubbling nitrogen, a higher current density is needed to reach the transition time with respect to the absence of bubbling nitrogen in order to increase the polarization concentration.

A significant number of systematic studies [4, 17, 18] on the deposition of metal powder have shown that the current density,  $i_p$ , for powder formation at which the transition from a compact to a powdery deposit occurs, corresponds to the limiting current density,  $i_l$  and there is a good agreement between the concentration dependence and Nusselt numbers. Therefore, it is reasonable to assume that powder formation starts as the reaction layer at the electrode is totally depleted of depositing metal ions at the limiting current density. The transition to a deposition in powdery form occurs in the region of the potential plateau in galvanostatic transients or the plateau of the current–potential curve which corresponds to the limiting current. Powder formation requires the process to be operated at the limiting current for cobalt deposition. However, under such conditions, hydrogen evolution increases to produce a mass of  $\text{Co(OH)}_2$  in the powders. As a result, the range of current density for deposition of cobalt powders from 0.05M  $\text{CoCl}_2$  under bubbling nitrogen ( $30 \text{ ml min}^{-1}$ ) is  $10\text{--}20 \text{ mA cm}^{-2}$ , a very narrow range.

### 3.2. Reactive deposition of powdery cobalt in the presence of bubbling oxygen

#### 3.2.1. Characteristics of the reactive deposition of powdery cobalt

In our previous studies on the reactive deposition of cobalt, it has been found that the effect of oxygen reduction during the deposition is to form a  $\text{Co(OH)}_2$  colloid layer on the interfacial plane which is dynamically unstable because of its reaction with  $\text{HO}_2^-$ , produced by oxygen reduction and the sparging effect

of bubbling oxygen. The unique characteristics of the reactive deposition process are directly responsible for the formation of ultrafine ( $< 1 \mu\text{m}$ ) powders on the deposit. In addition, it has been found [11, 19] that for the deposition of cobalt from aqueous chloride solution, hydrogen evolution becomes the main reaction at approximately  $-1.1 \text{ V}$  versus SCE in the absence of oxygen, but beyond approximately  $-1.2 \text{ V}$  versus SCE in the presence of oxygen. This confirms that the formation of a  $\text{Co(OH)}_2$  colloid layer at the electrode surface inhibits hydrogen evolution in the deposition.

Fig. 4 gives the potential–time transients without correction of the ohmic drop for the initial deposition of cobalt powders from 0.05M  $\text{CoCl}_2$  solution in the presence of dissolved oxygen and bubbling oxygen ( $30 \text{ ml min}^{-1}$ ). The transients in the presence of dissolved oxygen show a similar characteristic to those in the presence of bubbling nitrogen or the absence of oxygen; the overpotential increased with time and finally reached a potential plateau at which the interfacial concentration of  $\text{Co}^{2+}$  ions falls to zero. However, even compared to the case of bubbling nitrogen ( $30 \text{ ml min}^{-1}$ ), the transition time to reach the potential plateau in the presence of dissolved oxygen is generally much longer. In the presence of oxygen during the electrodeposition, oxygen reduction takes place prior to the deposition of cobalt. According to Reaction 3, the  $\text{OH}^-$  formed in the oxygen reduction process reacts with  $\text{Co}^{2+}$  to form  $\text{Co(OH)}_2$ . Therefore, it acts as a pH buffer. Furthermore, the  $\text{Co(OH)}_2$  colloid layer inhibits the further increase in pH in the interfacial plane and depresses the hydrogen evolution reaction. Therefore, it is not surprising that the transition time for the deposition of cobalt in the presence and absence of oxygen is significantly different. On the other hand, the longer transition time in the presence of oxygen also means that the percentage of  $\text{Co(OH)}_2$  in cobalt powders may be lower and the current density applicable for powder formation may be higher.

On the other hand, the pH buffer effect of the  $\text{Co(OH)}_2$  colloid layer is also confirmed by potential

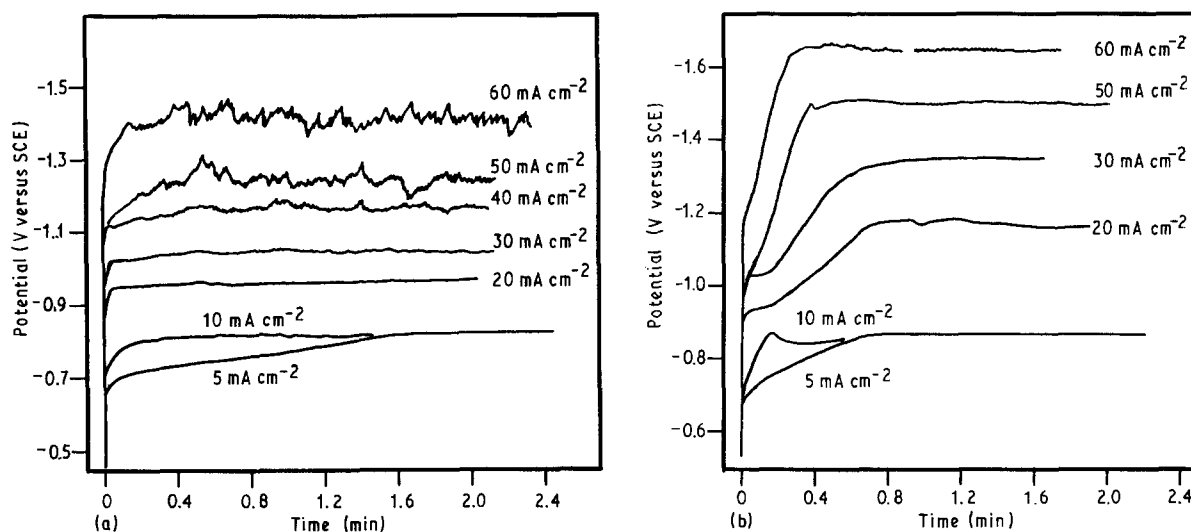


Figure 4 Potential–time transient curves without the correction of ohmic drop in the initial deposition obtained from 0.05M  $\text{CoCl}_2$  solution in the presence of (a) bubbling oxygen ( $30 \text{ ml min}^{-1}$ ) and (b) dissolved oxygen.

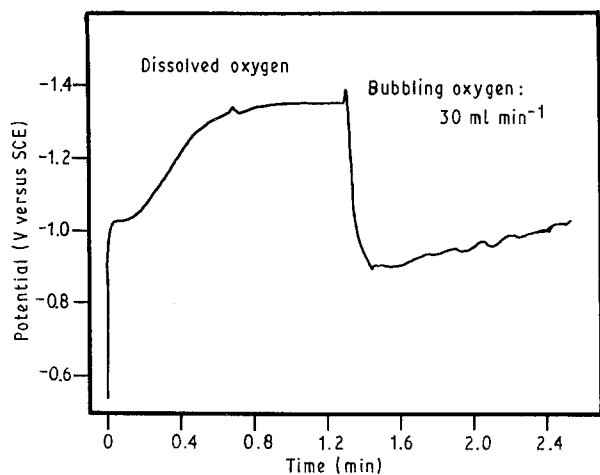


Figure 5 Potential-time transient curve obtained from 0.05M  $\text{CoCl}_2$  solution at a current density of  $30 \text{ mA cm}^{-2}$ .

changes on switching on and off the oxygen supply (Fig. 5). For the deposition of cobalt powder in the presence of dissolved oxygen at  $30 \text{ mA cm}^{-2}$ , hydrogen evolution is the dominant reaction at the potential plateau after the transition time; the overpotential immediately decreases once oxygen is fed into the solution continuously at a flow rate of  $30 \text{ ml min}^{-1}$ . This shows that a continuous  $\text{Co(OH)}_2$  colloid layer is formed due to the increase in oxygen reduction, which depresses the hydrogen evolution (via the increase in pH at the electrode surface), eliminates the formation of  $\text{Co(OH)}_2$  precipitate, and therefore results in the immediate drop of the overpotential. Although the sparging effect of bubbling oxygen on the mass transfer process cannot be ignored, it could obviously not cause such a significant decrease in the overpotential, because a simple sparging effect would only result in a drop in overvoltage similar to that for nitrogen sparging (Fig. 2).

It is interesting to note that there is a significant difference between the transients in the presence of dissolved oxygen (Fig. 4b) and the absence of oxygen (Fig. 2b). There is an extra plateau at the initial deposition time in the former case. This is particularly evident from the curves at moderate current densities of 20 and  $30 \text{ mA cm}^{-2}$  (Fig. 4b). After this extra plateau (first plateau), the overpotential continues to rise and then reach another plateau (second plateau) which corresponds to the plateau obtained in the absence of oxygen. In the presence of oxygen, the transition time to reach the first plateau is comparable to that required to reach the plateau in the absence of oxygen. This is due to the change in the structure of the electric double layer in the reactive deposition process resulting from the formation of the  $\text{Co(OH)}_2$  colloid layer at the electrode surface. Fig. 6 is a schematic diagram of the structure of the electric double layer for the reactive deposition of cobalt. In the presence of oxygen, due to the formation of  $\text{Co(OH)}_2$  colloid layer in the interfacial plane, the surface concentration of  $\text{Co}^{2+}$  ions quickly decreases and the mass transfer of  $\text{Co}^{2+}$  ions is through the  $\text{Co(OH)}_2$  colloid layer according to Reaction 3. This facilitates the formation of cobalt powder. Therefore,

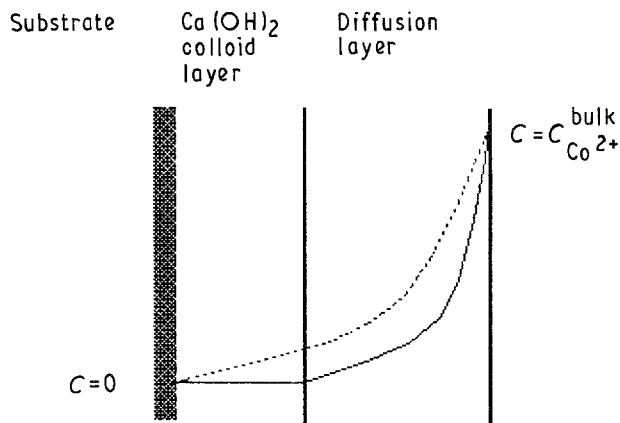


Figure 6 Schematic structure of the electric double layer in the reactive deposition of cobalt. (---) Change of  $\text{Co}^{2+}$  concentration in the absence of  $\text{Co(OH)}_2$  colloid layer.

the first transition time is much shorter in the presence of oxygen.

In the reactive deposition of cobalt, hydrogen evolution is a competitive process with the electrodeposition of cobalt and oxygen reduction. Oxygen reduction is under limiting diffusion control which depends on the concentration of oxygen dissolved in the solution. In the presence of dissolved oxygen (Fig. 4b), at current densities higher than  $30 \text{ mA cm}^{-2}$ , hydrogen evolution is the predominant reaction. Therefore, the first plateau disappears because of the breakdown of the  $\text{Co(OH)}_2$  colloid layer at the electrode surface. Similarly, due to the stirring effect of oxygen bubbles, current densities higher than  $40 \text{ mA cm}^{-2}$  are required for the first plateau to disappear (Fig. 4a). On the other hand, as shown in Fig. 4b, after some time, the  $\text{Co(OH)}_2$  colloid layer at the electrode surface is also broken and even disappears, accompanied by the depletion of dissolved oxygen in the solution. Moreover, in the reactive deposition of powdery cobalt, due to the stirring effect of oxygen bubbles and the continuous introduction of oxygen, at moderate current densities, the electrodeposition of cobalt can be the predominant process and the hydrogen evolution reaction is suppressed. For example, in 0.05M  $\text{CoCl}_2$  solution at a oxygen flow rate  $30 \text{ ml min}^{-1}$  (Fig. 4a) only the first plateau always exists at current densities lower than  $40 \text{ mA cm}^{-2}$  during the deposition. This shows that a higher deposition current density can be used at the same  $\text{Co}^{2+}$  concentration for the reactive deposition of cobalt than the normal electrodeposition, because the hydrogen evolution reaction is suppressed. This result is very important for the manufacture of electrolytic cobalt powders because the productive rate can be increased without significant production of  $\text{Co(OH)}_2$ .

The first and second transition time, respectively, measured in the presence of bubbling oxygen (Fig. 4b) and in the presence of dissolved oxygen (Fig. 4a) are plotted logarithmically against current density in Fig. 7. Two parallel straight lines with a slope of approximately  $-2$  are obtained as required by Equation 6, similar to the result obtained in the absence of oxygen (Fig. 3). The distortion of the

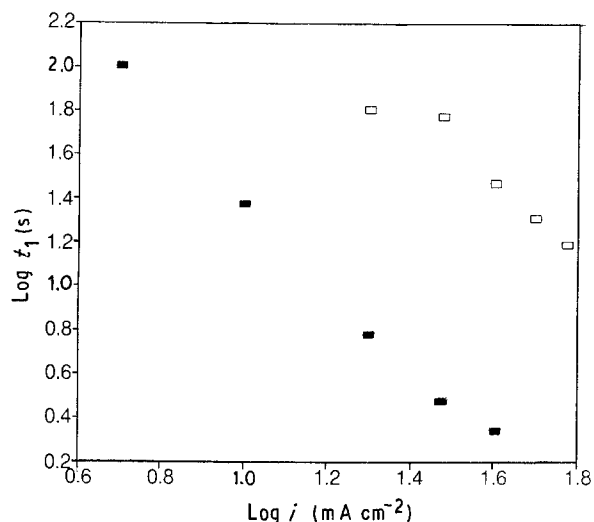


Figure 7 Logarithmical relationship of current with (■) first transition time in the presence of bubbling oxygen ( $30 \text{ ml min}^{-1}$ ) and □ second transition time in the presence of dissolved oxygen from  $0.05\text{M CoCl}_2$  solution.

transition time measured at current densities lower than  $30 \text{ mA cm}^{-2}$  from the straight line in the presence of dissolved oxygen in Fig. 7 is probably due to the significant decrease of oxygen concentration dissolved in the solution over such a long deposition time. Therefore, the results in Fig. 7 show that there are two limiting diffusion processes of  $\text{Co}^{2+}$  ions in the reactive deposition of cobalt. According to the structure of the electric double layer shown in Fig. 6, in the region of the first transition time, the current density is mainly contributed from the limiting mass transfer of  $\text{Co}^{2+}$  ions from bulk solution through the  $\text{Co(OH)}_2$  colloid layer, and the electro-deposition of cobalt is the predominant process. However, at a much higher current density, the  $\text{Co(OH)}_2$  colloid layer at the electrode surface is broken and disappears, cobalt is then deposited on to the substrate, via the limiting diffusion of  $\text{Co}^{2+}$  ions from the bulk solution to the surface. At this time, hydrogen evolution is a predominant reaction to reach the second plateau. Therefore, because the  $\text{Co(OH)}_2$  colloid layer is formed in the reactive deposition of cobalt, the limiting diffusion condition for the formation of cobalt powders is reached with the elimination of hydrogen evolution.

As a result, in the reactive deposition of cobalt powder in the presence of bubbling oxygen, the existence of the  $\text{Co(OH)}_2$  colloid layer not only inhibits the accompanying hydrogen evolution in the deposition, but also accelerates the decrease of the  $\text{Co}^{2+}$  concentration in the interfacial plane. Therefore, the reactive deposition of cobalt has the advantages of a lower ratio of  $\text{Co(OH)}_2$  in the cobalt powders and a wider range of current density for the powdery cobalt formation, compared to the normal electrodeposition of cobalt. At a moderate current density where the second transition could never be reached, the limiting condition (i.e. the formation of powdery cobalt) could be achieved with little hydrogen evolution, which is not possible for the deposition of cobalt in the absence

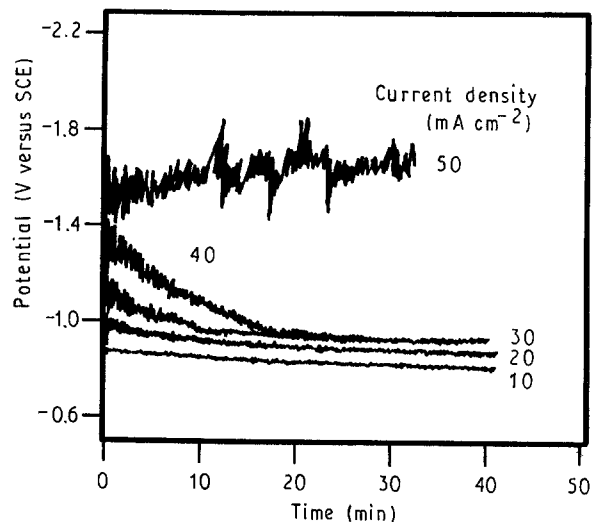


Figure 8 Potential-time transient curves obtained from  $0.05\text{M CoCl}_2$  solution in the presence of bubbling oxygen ( $30 \text{ ml min}^{-1}$ ) at different current densities.

of oxygen. As an illustration, it can be seen from Fig. 8 that the overpotential increases with time due to the production of a large amount of  $\text{Co(OH)}_2$  only when current density is higher than  $40 \text{ mA cm}^{-2}$ . This is the same as the result in Fig. 4b, where the second transition time occurs only when the current density is higher than  $40 \text{ mA cm}^{-2}$ . The suitable range of current density in the reactive deposition of powdery cobalt from  $0.05\text{M CoCl}_2$  solution in the presence of bubbling oxygen ( $30 \text{ ml min}^{-1}$ ) is  $5\text{--}40 \text{ mA cm}^{-2}$ , a much wider range than that obtained with the same conditions in the presence of bubbling nitrogen ( $30 \text{ ml min}^{-1}$ ).

### 3.2.2. Particle size of cobalt powders

In previous studies on the reactive deposition of cobalt electrode [11–13], it has been found that because of the formation of the  $\text{Co(OH)}_2$  colloid layer at the electrode surface and the change of its dynamic states prior to the deposition of cobalt, the reactive deposition of cobalt is characterized by localized nucleation and limited crystal growth processes. The  $\text{Co(OH)}_2$  colloid layer at the electrode depresses the nucleation potential of cobalt to the cathodic side. Individual cobalt particles could be isolated and their extensive crystal growth inhibited due to the continuous formation of a  $\text{Co(OH)}_2$  colloid layer around the grain boundaries [12, 20]. This results in the production of high surface-area and highly porous deposits having a structure of ultrafine micrograins with a similar size of micropores. Fig. 9 shows the surface morphologies of the powdery deposits by using scanning electron microscopy (SEM). However, it can be clearly seen from Fig. 9b that the size of the grains prepared in the presence of bubbling oxygen is about  $0.4\text{--}0.6 \mu\text{m}$  and at least three times smaller than those prepared in the presence of bubbling nitrogen (Fig. 9a). Therefore, the preliminary result confirms that ultrafine cobalt powders can be prepared by reactive deposition. The effect of the  $\text{Co(OH)}_2$  colloid layer in the reactive deposition

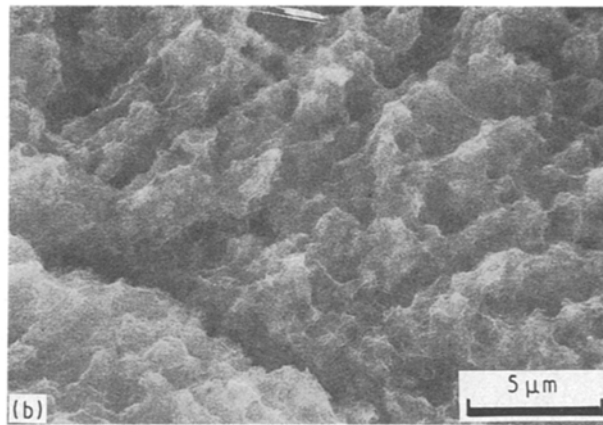
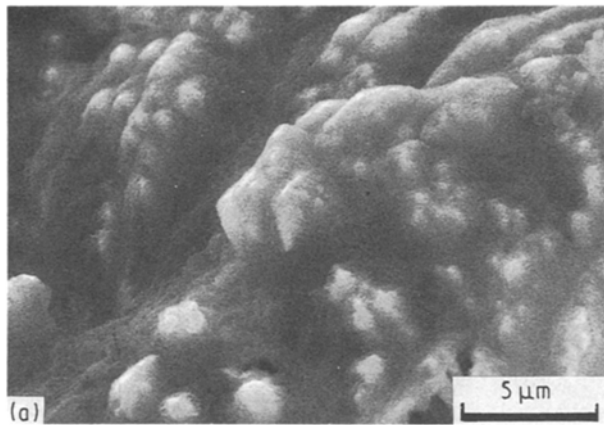


Figure 9 Surface morphologies of powdery cobalt deposits prepared from 0.05M  $\text{CoCl}_2$  solution on a titanium substrate at a current density of  $20 \text{ mA cm}^{-2}$  in the presence of (a) bubbling nitrogen ( $30 \text{ ml min}^{-1}$ ), and (b) bubbling oxygen ( $30 \text{ ml min}^{-1}$ ).

of cobalt powders is the same as in the reactive deposition of cobalt electrode, although the deposition kinetics is under limiting diffusion control.

### 3.2.3. Effects of $\text{CoCl}_2$ concentration in the solution and flow rate of bubbling oxygen

In our previous studies [12] on the reactive deposition of cobalt electrode, it has been shown that to produce high surface area deposits, the kinetics of cobalt deposition should be controlled by both diffusion and interfacial electron transfer processes. Moreover, the formation of a  $\text{Co(OH)}_2$  colloid layer is kinetically controlled by the oxygen reduction process which is mainly controlled by the concentration of dissolved oxygen in the solution. As the  $\text{Co}^{2+}$  concentration increases, the deposition of cobalt is predominantly via interfacial electron transfer control. Therefore, the inhibiting effect of the  $\text{Co(OH)}_2$  colloid layer is limited and a dense deposit is formed. As the deposition of cobalt is via diffusion control at low  $\text{Co}^{2+}$  concentration, a loose deposit is formed and the performance of the deposit as an electrode in the battery also decreased. In the reactive deposition of cobalt powders, the same effect of  $\text{Co}^{2+}$  concentration as in the reactive deposition of cobalt electrode is also seen in Fig. 10. In solutions containing dissolved oxygen at a given current density, it takes a longer transition time to reach the first potential plateau with the increase of  $\text{Co}^{2+}$  concentration.

In fact, the effect of the flow rate of bubbling oxygen on the kinetics of the cobalt deposition is similar to the effect of  $\text{Co}^{2+}$  concentration. When the flow rate of bubbling oxygen increases, for the deposition of powdery cobalt from 0.05M  $\text{CoCl}_2$  solution at a current density of  $60 \text{ mA cm}^{-2}$ , the potential-time transients are as shown in Fig. 11. At a lower flow rate of bubbling oxygen than  $60 \text{ ml min}^{-1}$ , the deposition of cobalt is greatly affected by hydrogen evolution and reaches a high potential plateau because of the formation of  $\text{Co(OH)}_2$  on the deposit. When the flow rate is higher than  $60 \text{ ml min}^{-1}$ , the second potential transition does not occur in the transients. Because oxygen reduction is under limiting diffusion control, the same

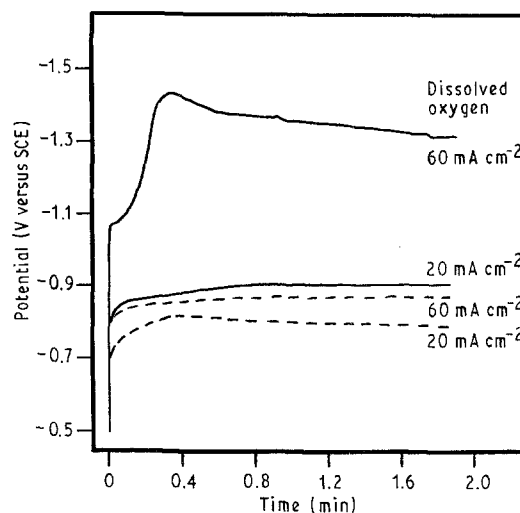


Figure 10 Potential-time transient curves obtained from (---) 0.1M  $\text{CoCl}_2$  solution and (—) 0.25M  $\text{CoCl}_2$  solution in the presence of dissolved oxygen.

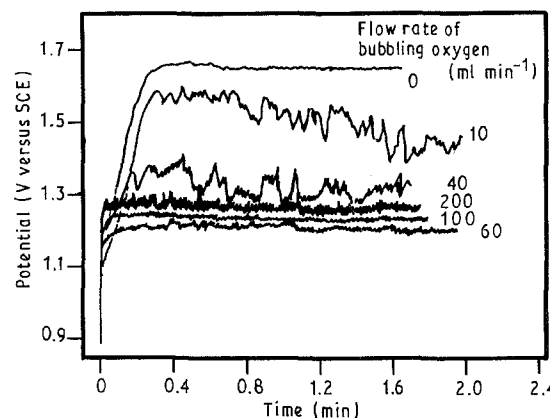


Figure 11 Potential-time transient curves obtained from 0.05M  $\text{CoCl}_2$  solution in the presence of bubbling oxygen with different flow rates at a current density of  $60 \text{ mA cm}^{-2}$ .

as the deposition of cobalt at high current densities, the sparging effect of bubbling oxygen is beneficial to the oxygen reduction reaction and the deposition of cobalt. Moreover, the effectiveness of the  $\text{Co(OH)}_2$  colloid layer is maintained, and this inhibits the competing process from the hydrogen evolution reaction.

Therefore, the effect of the flow rate of bubbling oxygen on the deposition of powdery cobalt may be considered to be predominately due to its sparging effect on the solution. On the other hand, in Fig. 8 the increase of overpotential at a flow rate of over 100 ml min<sup>-1</sup> than at 60 ml min<sup>-1</sup> is probably due to the decrease of the conductivity of the solution, due to the increased number of oxygen bubbles in the solution.

In the electrodeposition of powdery metals, the particle size of the metal powder increases with the concentration of metal ions, rate of stirring, and operating temperature. In fact, the changes in particle size can be best interpreted in terms of mass transfer phenomena. Therefore, in reactive deposition, the effects of the Co<sup>2+</sup> concentration and the flow rate of bubbling oxygen on the deposition of powdery cobalt are inter-related and predominantly due to their effect on the mass transfer process. Therefore, the reactive deposition of powdery cobalt has the same rule as the normal deposition of powdery metals, although the Co(OH)<sub>2</sub> colloid layer exists at the electrode surface. In practical applications, these factors can be adjusted to optimize the powdery deposition process.

#### 4. Conclusions

In the reactive deposition of cobalt powders, the formation of a Co(OH)<sub>2</sub> colloid layer at the electrode surface results in localized nucleation and a limited crystal growth process. Individual cobalt crystals are isolated by the Co(OH)<sub>2</sub> colloid at the grain boundaries to inhibit their growth and to produce ultrafine crystal grains, as in the reactive deposition of the cobalt electrode. On the other hand, the existence of the Co(OH)<sub>2</sub> colloid layer at the electrode depresses the hydrogen evolution reaction during the deposition process and accelerates the increase in interfacial Co<sup>2+</sup> concentration. Compared to the normal electrolytic preparation of cobalt powders, reactive deposition for the deposition of cobalt powders has the following advantages:

1. ultrafine cobalt powders (0.4–0.6 μm) can be manufactured;
2. hydrogen evolution in the deposition is depressed so that the amount of Co(OH)<sub>2</sub> in the powders decreases;
3. a wider range of current density for the formation of the powder can be used.

#### Acknowledgement

The experimental work was carried out at the Chemical Energy Research Centre (CERC), University of Essex, UK.

#### References

1. J. L. SU, M.-M. CHEN, J. LO and R. E. LEE, *J. Appl. Phys.* **63** (1988) 4022.
2. H. F. QUINN and L. M. CROLL, "Advances in X-ray Analysis" Vol. 4 (Plenum Press, New York, 1980), p. 151.
3. The Cobalt Development Institute (CDI), *Cobalt News* **89/2** (London 1989) p. 2.
4. N. IBL, in "Advances in Electrochemistry and Electrochemical Engineering", Vol. 2 edited by C. W. Tobias (Wiley, New York, 1962) p. 49.
5. K. AOTANI and D. KAGAKU, *J. Electrochem. Soc. J* **18** (1950) 323.
6. A. C. C. TSEUNG, S. P. JIANG, Y. Z. CHEN and J. K. YOU, Brit. Provisional Pat. Appl. 88, 154943, 29 June 1988.
7. A. C. C. TSEUNG, S. P. JIANG, Y. Z. CHEN, and J. K. YOU, *J. Mater. Sci. Lett.* **9** (1990) 1294.
8. S. P. JIANG, Y. Z. CHEN, J. K. YOU, T. X. CHEN and A. C. C. TSEUNG, *J. Electrochem. Soc.* **137** (1990) 3374.
9. S. P. JIANG and A. C. C. TSEUNG, *ibid.* **137** (1990) 3381.
10. *Idem, ibid.* **137** (1990) 3387.
11. S. P. JIANG, C. Q. CUI and A. C. C. TSEUNG, *ibid.* **138** (1991) 3599.
12. C. Q. CUI, S. P. JIANG and A. C. C. TSEUNG, *ibid.* **139** (1992) 60.
13. *Idem, ibid.* **139** (1992).
14. S. P. JIANG, C. Q. CUI and A. C. C. TSEUNG, *J. Mater. Sci.* **26** (1991).
15. N. IBL, R. KELLER and K. KILLER, in "Proceedings of the International Committee on Electrochemistry Thermodynamics and Kinetics (CITCE), 9th Meeting (Butterworths, London, 1959) p. 283.
16. G. WRANGLIN, *J. Electrochem. Soc.* **97** (1950) 353.
17. R. AOGAKI and T. MAKINO, *Electrochim Acta* **26** (1981) 1509.
18. A. R. DESPIC and K. I. POPOV, in "Modern Aspects of Electrochemistry", Vol. 7 edited by B. E. Conway and J. O' M. Bockris (Plenum Press, New York, 1972) p. 199.
19. C. Q. CUI, S. P. JIANG and A. C. C. TSEUNG, *J. Electrochem. Soc.* **137** (1990) 3148.
20. M. MIYATA, K. KOBAYASHI, H. WAKAYAMA, T. MIYABAYASHI, M. YASUDA and F. HINE, *Surface Technol.* **40** (1989) 472 (in Japanese).

Received 13 November 1991  
and accepted 24 March 1992